

LEPTOQUARKS IN $e^- \gamma$ COLLISIONS

FRANK CUYPERS

cuypers@pss058.psi.ch

Max-Planck-Institut für Physik, Föhringer Ring 6, D-80805 München, Germany

We discuss the leptoquark discovery potential of $e^- \gamma$ scattering and show how polarization and angular distributions can be used to differentiate the different types of leptoquarks.

The best present bounds on leptoquarks still originate from low energy experiments¹, and the constraints on flavour diagonal couplings are weak, at best. Some improvement is expected from HERA², but the real breakthrough should be obtained in high energy experiments of the next generation³. A particularly promising option is a linear collider operated in the $e^- \gamma$ mode⁴, where leptoquarks can be produced singly and very well studied.

Since leptoquarks appear in a wealth of extensions of the standard model, ranging from grand unified to composite models, it is important to perform an analysis which is as model-independent as possible. A general classification of these states, which respects $SU(3)_c \otimes SU(2)_L \otimes U(1)_Y$ invariance, was performed in Ref.². It assumes that, by definition, they couple to leptons and quarks, and must, therefore, be either singlets, doublets or triplets of the weak gauge group $SU(2)_L$. Also, for simplicity, only lowest dimension operators are involved, hence their couplings to leptons and quarks do not involve derivatives. Finally, in order not to induce rapid proton decay or other nuisances, they must conserve lepton (L) and baryon (B) number separately. The most general effective lagrangian which respects these conditions reads²

$$\begin{aligned}
L = & (h_{2L} \bar{u}_R \ell_L + h_{2R} \bar{q}_L i \sigma_2 e_R) R_2 + \tilde{h}_{2L} \bar{d}_R \ell_L \tilde{R}_2 + h_{3L} \bar{q}_L \boldsymbol{\sigma} \gamma^\mu \ell_L \mathbf{U}_{3\mu} \quad (1) \\
& + (h_{1L} \bar{q}_L \gamma^\mu \ell_L + h_{1R} \bar{d}_R \gamma^\mu e_R) U_{1\mu} + \tilde{h}_{1R} \bar{u}_R \gamma^\mu e_R \tilde{U}_{1\mu} \\
& + (g_{1L} \bar{q}_L^c i \sigma_2 \ell_L + g_{1R} \bar{u}_R^c e_R) S_1 + \tilde{g}_{1R} \bar{d}_R^c e_R \tilde{S}_1 + g_{3L} \bar{q}_L^c i \sigma_2 \boldsymbol{\sigma} \ell_L \mathbf{S}_3 \\
& + (g_{2L} \bar{d}_R^c \gamma^\mu \ell_L + g_{2R} \bar{q}_L^c \gamma^\mu e_R) V_{2\mu} + \tilde{g}_{2L} \bar{u}_R^c \gamma^\mu \ell_L \tilde{V}_{2\mu} + \text{h.c.} ,
\end{aligned}$$

where the $\boldsymbol{\sigma}$'s are Pauli matrices, while q_L and ℓ_L are the $SU(2)_L$ quark and lepton doublets and u_R , d_R , ℓ_R are the corresponding singlets. The subscripts of the leptoquarks indicates the size of the $SU(2)_L$ representation to which they belong. The R - and S -type leptoquarks are spacetime scalars, whereas the U and V are vectors. All family and colour indices are implicit.

Since all these leptoquarks carry an electric charge, they must also couple to the photon. These interactions are described by the kinetic lagrangians for

scalar and vector bosons

$$\mathcal{L}_{J=0} = \sum_{\text{scalars}} (D_\mu \Phi)^\dagger (D^\mu \Phi) - m^2 \Phi^\dagger \Phi \quad (2)$$

$$\mathcal{L}_{J=1} = \sum_{\text{vectors}} -\frac{1}{2} (D_\mu \Phi^\nu - D_\nu \Phi^\mu)^\dagger (D^\mu \Phi_\nu - D^\nu \Phi_\mu) + m^2 \Phi_\mu^\dagger \Phi^\mu \quad (3)$$

where Φ and A are the leptoquark and photon fields, $D_\mu = \partial_\mu - ieQA_\mu$ is the covariant derivative, e is the electromagnetic coupling constant and m and Q are the leptoquark mass and electromagnetic charge. This lagrangian describes the minimal vector boson coupling, typical of a composite leptoquark. If, however, the vector leptoquarks are gauge bosons, an extra Yang-Mills piece has to be added in order to maintain gauge invariance:

$$\mathcal{L}_G = \sum_{\text{vectors}} -ie \Phi_\mu^\dagger \Phi_\nu (\partial^\mu A^\nu - \partial^\nu A^\mu) . \quad (4)$$

If this piece is not included, tree-level unitarity is bound to be lost. Indeed, the effective lagrangian (3) is no longer valid at energies of the order of the scale where the full (gauge) theory from which it was derived has to be considered.

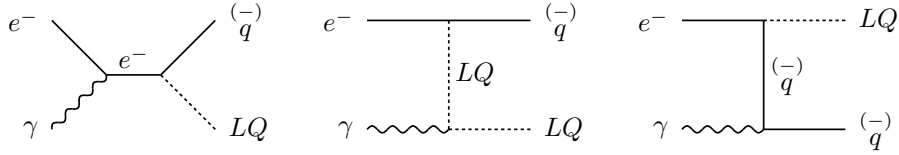


Figure 1: Lowest order Feynman diagrams for the production of leptoquarks.

Ignoring the resolved photon contributions the typical s -, t - and u -channel Feynman diagrams for the $e^- \gamma \rightarrow q LQ$ reaction are shown in Fig. 1. There are 24 different types of processes, depending on whether the produced leptoquark is a scalar, vector or gauge boson, whether it couples to right- or left-handed leptons and what is its electromagnetic charge ($Q = -1/3, -2/3, -4/3, -5/3$). We display the energy behaviour of the production cross sections in Fig. 2. For the purpose of these plots, we have set the generic leptoquark-electron-quark coupling λ equal to the electromagnetic coupling constant $\lambda = e$. As in the rest of this report, we also assume the electron and photon beams to be both 100 % polarized and monochromatic. A more detailed analysis, with realistic polarizations and energy spectra⁵, can be found in the last of Refs⁴.

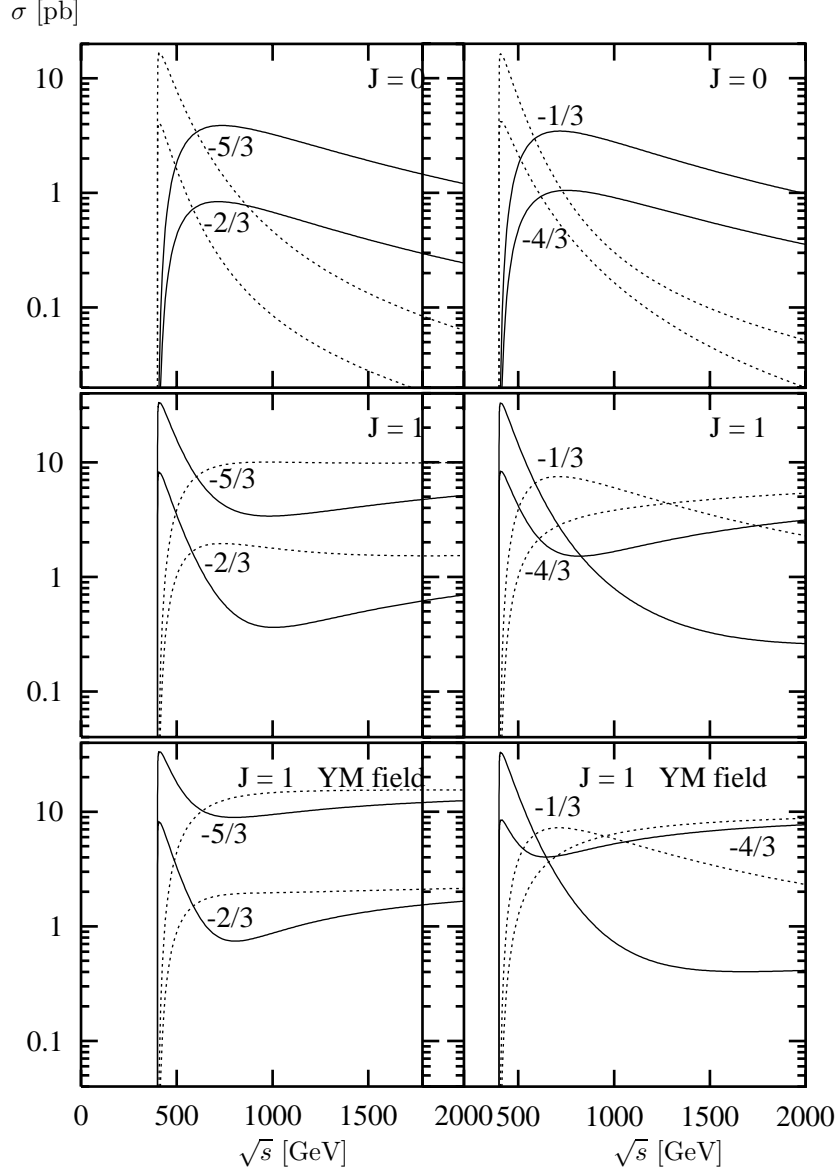


Figure 2: Energy dependence of 400 GeV leptoquark production cross sections. The solid curves correspond to the choice of respective electron and photon polarizations yielding $P_e P_\gamma = 1$, whereas the dotted curves are for $P_e P_\gamma = -1$. The charges of the leptoquarks are indicated next to the corresponding curves.

The threshold behaviour of the cross sections mainly depends on the u -channel singularity of the third graph in Fig. 1 and on the electron and photon relative polarizations:

$$\begin{cases} \sigma(J=0) & \propto & (1+Q)^2 & (1 \mp P_\gamma)(1 \pm P_e) \\ \sigma(J=1) & \propto & 2(1+Q)^2 & (1 \pm P_\gamma)(1 \pm P_e) \end{cases} \quad (5)$$

where P_e and P_γ are the polarizations of the electron and photon beams. The scalar cross sections quickly drop to zero for initial state electrons and photons with the same helicity, whereas the vector cross sections are suppressed when they have opposite helicities. For equal couplings, the vector threshold cross sections are twice as large as the scalar ones.

In the asymptotic region the $J=0$ and $J=1$ leptoquarks also display very different behaviours. Whereas the scalar cross sections decrease like $1/s$, the vector cross sections eventually increase like $\ln s$. If the vectors are gauge fields, though, their cross sections saturate for large values of s .

In general, the leptoquarks decay into a charged lepton and a jet with a substantial branching ratio. Even if the lepton is an electron, the standard model background can easily be rendered harmless by simple invariant mass cuts. To estimate the leptoquark discovery potential of $e^-\gamma$ collisions, we have plotted in Fig. 3 the boundary in the $(m_{LQ}, \lambda/e)$ plane, below which the cross section of a $Q = -5/3$ Yang-Mills leptoquark yields less than 10 events. For this we consider four different collider energies and assume 10 fb^{-1} of accumulated luminosity. In general, these curves are approximately osculated by the line

$$\frac{\lambda}{e} = 0.02 \frac{m/\text{TeV}}{\sqrt{\mathcal{L}/\text{fb}^{-1}}} \sqrt{\frac{n}{(J+1)(1+Q)^2}} \quad (m \leq .9\sqrt{s}) \quad , \quad (6)$$

where λ is the leptoquark's coupling to leptons and quarks, m its mass, Q its charge, J its spin, n is the required number of events and \mathcal{L} is the available luminosity. This scaling relation provides a convenient means to gauge the leptoquark discovery potential of $e^-\gamma$ scattering. It is valid for leptoquark masses short off 90% of the collider energy and assumes the electron and photon beams to be 100% polarized while their relative helicities are chosen such as to enhance the threshold cross section (*cf.* Eqs (5)).

In comparison, the best bounds on the leptoquark couplings, which have been derived indirectly from low energy data¹, are no better than

$$\frac{\lambda}{e} \geq m/\text{TeV} \quad , \quad (7)$$

for leptoquark interactions involving only the first generation. Similar bounds on couplings involving higher generations are even poorer.

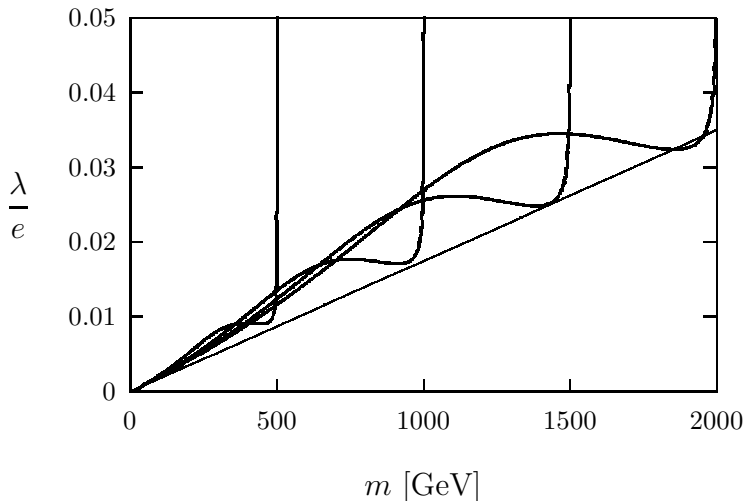


Figure 3: Loci of $\sigma(J = 1, Q = -5/3) = 1$ fb as a function of the leptoquark mass and coupling to fermions. The collider energies are from left to right .5, 1, 1.5 and 2 TeV and $P_e P_\gamma = 1$. The thinner oscillating line is given by Eq. (6).

If a leptoquark is discovered someday, it becomes interesting to determine its nature. In principle, $e^- \gamma$ scattering may discriminate between the 24 combinations of the quantum numbers J , Q and P , where the latter is the chirality of the electron to which the leptoquark couples. For the case $J = 1$ we make the distinction between gauge and non-gauge leptoquarks.

It is of course trivial to determine P by switching the polarization of the electron beam. Similarly, it is almost as easy to distinguish scalars from vectors. Indeed, as can be inferred from Eqs (5) and from Fig. 2, all threshold cross sections are very sensitive to the relative electron and photon polarizations. Since this effect works in opposite directions for $J = 0$ and $J = 1$, a simple photon polarization flip upon discovery should suffice to determine the spin of the discovered leptoquarks.

To determine the other quantum numbers, we turn to the differential distributions. As it turns out, the interferences between the different channels result into rather complex angular dependences of the cross sections. There are even radiation zeros for the reactions involving scalar and Yang-Mills leptoquarks of charges $-1/3$ and $-2/3$.

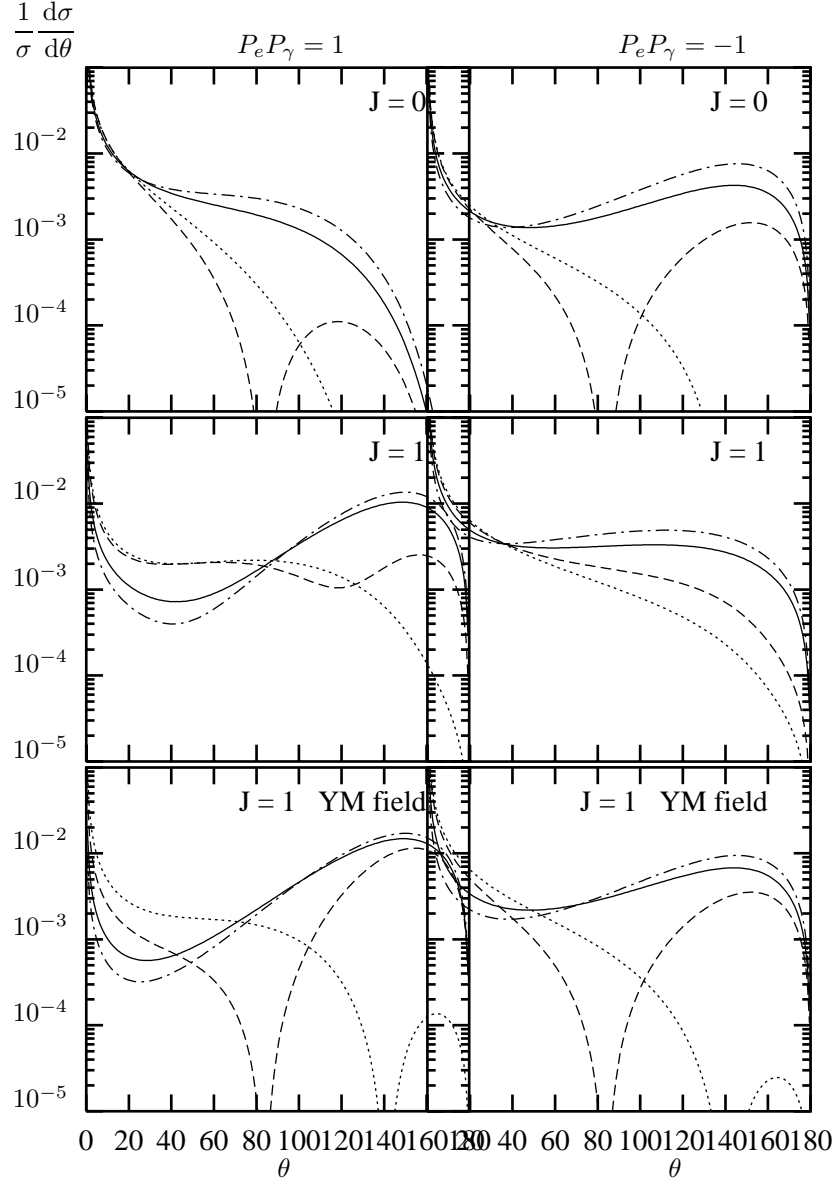


Figure 4: Angular distributions of 500 GeV leptoquarks produced in 1 TeV collisions. The coding of the curves is solid: $Q = -5/3$; dot-dashed: $Q = -4/3$; dashed: $Q = -2/3$; dotted: $Q = -1/3$.

These very salient features are displayed in Fig. 4 and could well be observed away from threshold, where the u -channel pole is no longer so dominant. In this figure, we have considered 500 GeV leptoquarks produced at a 1 TeV collider.

$\frac{\lambda}{e}\sqrt{\mathcal{L}/\text{fb}^{-1}}$		$J = 0$			
		$-\frac{5}{3}$	$-\frac{2}{3}$	$-\frac{4}{3}$	$-\frac{1}{3}$
$J = 0$	$-\frac{5}{3}$	\times	.2	.6	.2
	$-\frac{2}{3}$.6	\times	.5	2.1
	$-\frac{4}{3}$.9	.2	\times	.2
	$-\frac{1}{3}$.3	1.0	.2	\times

$\frac{\lambda}{e}\sqrt{\mathcal{L}/\text{fb}^{-1}}$		$J = 1$				$J = 1$ YM field			
		$-\frac{5}{3}$	$-\frac{2}{3}$	$-\frac{4}{3}$	$-\frac{1}{3}$	$-\frac{5}{3}$	$-\frac{2}{3}$	$-\frac{4}{3}$	$-\frac{1}{3}$
$J = 1$	$-\frac{5}{3}$	\times	.2	.7	.2	.3	.2	.2	.1
	$-\frac{2}{3}$.6	\times	.6	1.0	.4	.4	.3	.6
	$-\frac{4}{3}$	1.0	.3	\times	.2	.5	.3	.4	.2
	$-\frac{1}{3}$.3	.6	.2	\times	.2	.2	.2	.8
$J = 1$ YM field	$-\frac{5}{3}$.2	.07	.2	.07	\times	.2	.7	.06
	$-\frac{2}{3}$.6	.4	.5	.3	.7	\times	.6	.3
	$-\frac{4}{3}$.2	.09	.2	.09	1.0	.2	\times	.08
	$-\frac{1}{3}$.2	.4	.2	.9	.2	.2	.2	\times

Table 1: Smallest values of $\lambda/e\sqrt{\mathcal{L}/\text{fb}^{-1}}$ which allow discriminating with 99.9% confidence two different 500 GeV scalar or vector leptoquarks at a 1 TeV collider. Scalar and vector leptoquarks can easily be told apart by flipping the laser polarization at threshold. The charge of the leptoquarks is listed in the second row and column. The leptoquarks listed in the rows are assumed to produce the data, whereas those listed in the columns are tested against this data.

To roughly estimate the $e^- \gamma$ potential for discriminating the different types of leptoquarks, we compare these differential distributions with a Kolmogorov-Smirnov test. Focusing on the case of Fig. 4, where a 500 GeV leptoquark is

